A study of hydrodynamics and interfacial momentum exchange terms in cylindrical bubble column by CFD
Proceedings of European Congress of Chemical Engineering (ECCE-6)
Copenhagen, 16-20 September 2007

A study of hydrodynamics and interfacial momentum exchange terms in cylindrical bubble column by CFD

M. R., Kamali, [a] A. Laari, [a] I. Turunen [a]

[a]*Lappeenranta University of Technology, Department of Chemical Technology, Laboratory of Process and Product Development, PO. Box 20, FIN-53851, Lappeenranta, Finland, kamali@lut.fi, arto.laari@lut.fi, ilkka.turunen@lut.fi.*

Abstract

Flow fields and bubble size distribution are two critical issues in the determination of mass transfer and reaction rate in bubble columns. In this work the hydrodynamics of bubble driven flow was investigated in a laboratory scale cylindrical bubble column. The column was a semi batch reactor which was initially filled with tap water and only gas was evenly fed to the column from the bottom with different flow rates. The simulations were carried out by using Eulerian-Eulerian multiphase approach in ANSYS CFX-10. Population balances for different discretized bubble size groups were solved by using the MUSIG model and by considering the Prince and Blanch (1990) and Luo and Svendsen (1996) models for coalescence and breakage models, respectively. Proper interfacial momentum exchange closures were found by comparing the simulation results with experiments. The simulated time averaged liquid, slip and bubble velocity distributions in the column accompanied by turbulent kinetic energy distribution were validated by experimental data obtained by Particle Image Velocimetry (PIV) measurements in the same conditions. Moreover, the validated models were used to predict gas hold up, bubble size and interfacial area distribution for the same column. The effect of the inlet superficial gas velocity on simulations was also investigated.

Keywords: bubble column, hydrodynamics, CFD, interfacial momentum exchange, MUSIG.

1. Introduction

Good mass and heat transfer characteristics, simple construction and low operating costs have made bubble columns a popular type of gas liquid reactors in a variety of industries.

Gas-liquid interfacial area is one of the critical variables in bubble column operation since it affects mass transfer and reaction rate in the column. This variable can be calculated using the bubble size distribution in the column and it is extremely dependent on the hydrodynamics of the system. Even though there has been a lot of research about this topic, the fluid behaviour in bubble column is still not fully understood.

In recent years, CFD has become a favourite topic for the analysis of fluid mechanics in multiphase systems such as bubble columns. Euler-Euler [Krishna et al. 1999 ; Pan et al. 1999; Sokolichin and Eigenberger, 1999; Torvik and Svendsen,1990]and Euler-Lagrange [Delnoij et al. 1997; Sokolichin et al. 1997; Van den Hengel et al. 2005; Darmana et al., 2005] are two commonly used distinct models for the CFD simulation of flow in this type of equipment. Among these two, Euler-Euler approach has shown to be numerically more efficient than the alternative Euler-Lagrange model particularly in the domains with high concentration of dispersed phase [Wiemann 2005]. Therefore, Euler-Euler model was used in the current work. This model is based on the solution of the ensemble-averaged Navier-Stokes equations for each phase with their distinctive flow properties.

To qualify CFD simulations for bubbly flow with Euler-Euler approach, it is necessary to consider interaction between the gaseous and liquid phase. This interaction usually concerns forces acting on the bubbles and bubble coalescence and breakage.

The forces that act on the bubbles are included in the Eulerian momentum equation as interfacial momentum exchange terms. Drag, lift, virtual mass, wall lubrication and turbulent dispersion forces are some of these important interaction terms. These terms have strong effect on the evolution of flow pattern in cylindrical bubble column which is classified as bubble driven flow. In these systems, drag is the main momentum exchange term in the direction of the flow and it can affect many things such as the liquid velocity profile. On the other side, the lift force mostly acts perpendicular to the flow direction and can determine the radial distribution of the bubbles. [Krepper et al. 2004]. In addition, the wall lubrication, virtual mass and turbulence dispersion forces are other factors which can affect the numerical simulation as well.

Usually interfacial momentum exchange terms should be adjusted together simultaneously. This is due to their complex dependency on the bubble size and shape, liquid flow field and material properties [Zhang, 2006]. A correct combination of these forces has great influence on the numerical simulations of bubbly flow. In

spite of many efforts inn finding a good interfacial closure [Clift et al., 1978; Ishi and Zuber, 1979; Jakobsen et al., 1997; Tomiyama, 2004] it still remains a challenging topic for many researchers [Zhang, 2006]. These efforts have lead to proposing some experimental closures. However, suggested closures seem not to be universal and their performance depends on the studied systems.

Many investigations show that bubble size distribution is an important factor in the formulation of interfacial forces [Jakobsen, 1997; Krepper, 2004; Tomiyama, 2004;]. This dependency is more crucial for the drag and lift forces [Jakobsen, 1997; Lucas et al., 2001; Tomiyama et al. 1998; Krepper, 2004]. However, there are some size dependent correlations for other forces as well. In the most of the CFD simulations constant bubble size is used in the calculation instead of variable distribution. This simplification limits such simulations to the homogenous regime and neglects many important interactions in the calculations. Due to importance of the bubble size in the simulations, it is necessary to solve the population balance equations coupled with CFD. This can be done by using either discretization or moment methods [Sha et al., 2006]. Only discretization methods are considered in this work. The Multi Size Group (MUSIG) model in ANSYS CFX 10 is one of these methods. In this approach it is assumed that there are different bubble size classes in the domain and that all the bubble size classes share the common velocity field. Bubble size distribution can be found through number conservation of each class considering coalescence and breakup models. [Lo, 1996; Buwa and Ranade, 2002]. As mentioned by Krishna et al. 2000, Lehr et al. 2002 and Sha et al. 2005 it is more accurate to consider more than one dispersed phase in the MUSIG type of simulation. This approach, called as Multi-Phase-Multi-Size group model, was implemented and tested by Sha et al. (2006).

In the current work simulated flow fields obtained by using different interfacial closures are compared with experimental results to find efficient models. Besides of comparison of available Tomiyama (2004) and Ishii and Zuber (1979) models, a new closure is proposed based on experimental data from different authors. In order to consider bubble size distribution in the interfacial force formulations, the MUSIG model was used. The Prince and Blanch (1990) and Luo and Svendsen (1996) models were used as the coalescence and breakage models, respectively.

2. Mathematical Models

As previously described, in Euler-Euler approach mass and momentum conservation laws are solved for each phase separately and they are based on ensemble- averaged quantities. In this approach the bubble flow hydrodynamics in the calculation is based on some assumptions. It is assumed that flow conditions are isothermal; there is no mass transfer between the continuous and the dispersed phases; liquid density is constant and gas density for different bubble classes depends on local pressure as described by the ideal gas law.

2.1. Continuity equations

Since there is no mass transfer between gas and liquid, the continuity equation for each phase can be formulated without any additional mass-transfer term between the dispersed and the continuous phase. However, mass transfer between the different classes of the dispersed phase should be considered in the governing equations. Thus, the continuity equation for the liquid and gas can be expressed as equations 1 and 2:

$$\frac{\partial}{\partial t}(\alpha_l \rho_l) + \nabla \bullet (\alpha_l \rho_l U_l) = 0 \tag{1}$$

$$\frac{\partial}{\partial t}(\alpha_g f_i \rho_g) + \nabla \bullet (\alpha_g f_i \rho_g U_g) = S_i \tag{2}$$

2.2. Momentum equations

The momentum equation for both phases (k = liquid or gas) can be formulated as Eq. 3.

$$\frac{\partial}{\partial t}(\alpha_k \rho_k U_k) + \nabla \bullet (\alpha_k \rho_k U_k U_k - \alpha_k \mu_{eff,k}(\nabla U_k + (\nabla U_k)^T)) = \alpha_k (\rho_k g - \nabla p) + M_k \tag{3}$$

In this equation $\mu_{eff,k}$ is the effective viscosity and it is related to the turbulence models.

2.3. Interfacial momentum exchange terms

M_k in Eq. 3 is the momentum exchange term which can be defined as follows:

$$M_k = M_k^{Drag} + M_k^{Lift} + M_k^{VM} + M_k^{WL} + M_k^{TDF} \tag{4}$$

The right hand side terms of this equation are the drag, lift, virtual mass, wall lubrication and turbulence dispersion forces, respectively. Even though, drag is the most important term the non-drag forces also have considerable effect on the simulations. For liquid and gas M_k has different sign. Each term in Eq.4 can be formulated by the following equations.

The first contributor is the drag force, which is formulated as follows:

$$M_l^{Drag} = \frac{3}{4}\rho_l \frac{\alpha_g}{d_{32}} C_D (U_g - U_l)\left|U_g - U_l\right| \tag{5}$$

The drag force acts in the direction of bubble movement. This force is a combination of the friction and pressure forces on the bubble. The former acts in the direction parallel to the bubble surface and the latter in the perpendicular one. Drag has crucial effect on the hydrodynamics of the system especially on the velocity vectors. A bubble that moves relative to the liquid accelerates part of the surrounding liquid and decelerates itself. Therefore, it can intensively change the velocity field as an important contributor.

There have been various proposals for the drag model. Each of these models is valid in appropriate conditions. For air-water system, the Grace (1978) and Ishii and Zuber (1979) models are widely used. Both of these models are explicitly dependent on the gravity vector and on the surface tension. The volume fraction of the gas and the interaction of the bubbles in the domain can change the applicability of these models. There are some drawbacks in using these models. In the current study it was found that the Grace model could not predict a physically acceptable flow field. Whereas, the Ishii and Zuber model could do that in some extent. In the current study, other models which could reliably predict the fields have been investigated.

Finding a reliable drag coefficient for the bubbly flow has been a challenging topic studied in several articles [Sokolichin, 2004]. The importance of the drag model is due to its cruicial effect on the hydrodynamics. The drag coefficient depends on the bubble Reynolds number, Eotvos number and Morton or Weber number. The derivation of reliable empirical correlations for the drag coefficient (C_D) is complicated by the fact that a direct measurement of the drag force acting on a gas bubble is possible only for the terminal rise velocity of a single air bubble in stagnant liquid. Impurities in the liquid have important effect on the drag coefficient. In fact, bubble rise velocity depends strongly on the purity of water or liquid [Jacobsen 1997]. In the current study 3 different correlations for (C_D) were used in different interfacial closures.

Another important term in Eq. 4 is the lift force. The lift force acts perpendicular to the direction of the relative motion of the two phases. It is an important force for the radial distribution of the bubbles. Lift contributes in the momentum equation by Eq.6.

$$M_l^{Lift} = \alpha_g \rho_l C_L \left(U_g - U_l\right) \times \mathrm{curl}(U_l) \tag{6}$$

The lift force acts in a different way depending on the bubble size. For small bubbles (d_B< 5.5 mm) it pushes the bubbles to the regions with lower liquid velocity i.e. towards the wall. For larger bubbles it acts in the opposite direction pushing large bubbles to high velocity regions in the centre of the column.

Appart from the above mentioned forces the virtual mass force seems to have the least effect on the hydrodynamics of the current system. This force depends on the relative phasic acceleration as presented in Eq.7.

$$M_l^{VM} = \alpha_g \rho_l C_{VM} \left(\frac{D_g U_g}{D_t} - \frac{D_g U_l}{D_t} \right) \tag{7}$$

Laurrien et al (2004) proposed the following correlation for the virtual mass coefficient in bubbly flow.

$$C_{VM} = 0.5 + 1.63\alpha_g + 3.85\alpha_g^2 \tag{8}$$

Including the virtual mass force to the model might increase computational load, which should be considered.

For wall lubrication force the Antal et al. (1991) model is used in the simulations in this work. This model can be formulated as Eq. 9.

$$M_l^{WL} = \alpha_g \rho_l \left| U_g - U_l \right|^2 \max\left(0, \frac{C_{w1}}{d_p} + \frac{C_{w2}}{y_w} \right) \tag{9}$$

Lopez de Bertodano (1991) proposed one of the first models for the turbulent dispersion force by Eq. 10.

$$M_{lg}^{TDF} = -C_{TDF} \rho_l k_l \nabla \alpha_l \tag{10}$$

There is no universal value for C_{TDF}, and it can vary depending on the case. However, in bubbly flow, where the bubble sizes are in the order of few millimetres, this value is between 0.1 and 0.5.

The interfacial momentum exchange terms have important effect on the simulation of bubbly flow. These terms can be tuned by using experimental coefficients obtained by comparing the simulations to experimental data. Three different closures have been investigated in the present work. These closures are shown in Table 1.

Table 1: Different investigated interfacial force closures

<table>
<tr><th>Closure A</th><th>Closure B (based on Tomiyama 2004)</th></tr>
<tr><td>$C_D = 0.2 + \frac{(d_{32} - 0.0015)^2}{0.42(d_{32} - 0.0015)^2 + 2.7\times10^{-6}}$
(Jacobsen et al. 1997 for Air/Tap water)

$C_L = \begin{cases} 0.06 & Eo < 4 \quad Krepper\ et\ al.,2005 \\ -0.1 & Eo \geq 4 \quad Sokolichin\ et\ al.,2004 \end{cases}$
$C_{w1} = -0.0064$
$C_{w2} = 0.016$ (Antal et al. 1991, Krepper et al. 2005)
$C_{TD} = 0.1$ (Lopez de Bertodano, 1991)
$C_{VM} = 0.3$
Turbulence Transfer model: Sato Enhanced model</td><td rowspan="2">$C_D = \frac{8Eo(1-E^2)}{3g(E)^2 E^{2/3} Eo + 16(1-E^2)E^{4/3}}$
$E = \frac{1}{1+0.163Eo^{0.757}}$
$Eo = \frac{g(\rho_l - \rho_g)d_b^2}{\sigma}$
$Eo_h = \frac{Eo}{E^{2/3}}$
$g(E) = \frac{\sin^{-1}\sqrt{1-E^2} - E\sqrt{1-E^2}}{1-E^2}$
$C_L = \begin{cases} \min[0.288\tanh(0.121\,\mathrm{Re}),\ f(Eo_h)] & Eo_h \text{ p } 4 \\ f(Eo_h) & 4 \leq Eo_h \leq 10 \\ -0.29 & Eo_h \text{ f } 10 \end{cases}$
$f(Eo_h) = 0.0010\,Eo_h^3 - 0.0159Eo_h^2 - 0.0204Eo_h + 0.474$
$C_{w1} = -0.0064$
$C_{w2} = 0.016$ (Antal et al. 1991, Krepper et al. 2005)
$C_{TD} = 0.1$ (Lopez de Bertodano, 1991)
$C_{VM} = 0.3$
Turbulence Transfer model: Sato Enhanced model</td></tr>
<tr><th>Closure C (based on Ishii-Zuber 1979)</th></tr>
<tr><td>$C_D = \frac{2}{3}\sqrt{Eo}$
$C_L = 0.5$
$C_{w1} = -0.0064$
$C_{w2} = 0.016$ (Antal et al. 1991, Krepper et al. 2005)
$C_{TD} = 0.1$ (Lopez de Bertodano, 1991)
$C_{VM} = 0.3$
Turbulence Transfer model: Sato Enhanced model</td></tr>
</table>

2.4. Turbulence models

For turbulence in the liquid phase the standard k-epsilon model was used. In addition, in bubble driven flows it is necessary to consider bubble induced turbulence which can affect the calculations significantly. This contribution was implemented by considering the enhanced model of Sato et al. (1975).

2.5. Population balance and MUSIG model

In order to solve the population balance equations, the dispersed phase will be considered as a poly-dispersed fluid and the bubble size is divided to a suitable number of bubble size classes (N_c). There are different bubble size discretization methods which can be used including the uniform discretization method used in the current work. According to this method the representative diameter of each size group is related to the minimum and maximum bubble diameters and N_c according to Eq. 11.

$$d_i = d_{min} + \left(\frac{d_{max} - d_{min}}{N_c} \right) \left(i - \frac{1}{2} \right) \tag{11}$$

Eq. 12 shows the population balance equation for the different bubble size classes of the dispersed phase.

$$\frac{\partial}{\partial t}(n_i \rho_g) + \nabla \bullet (n_i \rho_g U_g) = \rho_g (B_{Bi} - D_{Bi} + B_{Ci} - D_{Ci}) \tag{12}$$

where n_i is the population density, B_B and B_C are the birth rates due to break-up and coalescence respectively, and D_B and D_C the corresponding death rates.

Eq.12 can be rewritten by using the relationship between n_i and f_i (volume fraction).

$$n_i = \frac{6 f_i}{\pi d_i^3} \tag{13}$$

$$\frac{\partial}{\partial t}(f_i \rho_g) + \nabla \bullet (f_i \rho_g U_g) = \frac{\pi}{6} \rho_g d_i^3 (B_{Bi} - D_{Bi} + B_{Ci} - D_{Ci}) = S_i \tag{14}$$

There are Nc number of PBEs in the simulation domain which should be solved as scalar equations coupled with the Navier-Stokes equations. The solution of these PBE-CFD coupled equations can be done by different algorithms. In the current work the MUSIG model has been used. Even though this model has its own drawbacks it can still predict a reasonable bubble size distribution in the system. Details of this model are presented by Luo (1998).

The Sauter mean diameter, d_{32}, and the specific interfacial area, a, of the dispersed phase can be calculated from the group volume fractions and the corresponding bubble sizes. Eqs. 15, 16 are used in this respect.

$$d_{32} = \frac{\sum_{i=1}^{Nc} n_i d_i^3}{\sum_{i=1}^{Nc} n_i d_i^2} = \frac{1}{\sum f_i / d_i} \tag{15}$$

$$a = \frac{6 \alpha_g}{d_{32}} \tag{16}$$

According to Prince and Blanch (1990), coalescence can be modelled by considering bubble collision frequency and collision efficiency. The collision frequency has contributions from turbulence, buoyancy and laminar shear collision rates. The laminar shear collision rate is neglected in the available model in CFX and should be coded for some particular cases. In the Prince and Blanch model the different

coalescence properties of liquids are expressed by the time required for the film between the two colliding bubbles to thin and break. This film thinning time depends from the initial and critical thicknesses for the film. In the current study the values used for the initial and critical film thicknesses were 1×10^{-4} m and 1×10^{-8} m, respectively. More details of this model are available in the original article.

Luo and Svendsen (1996) developed a theoretical model for the breakup of drops and bubbles in turbulent suspensions. The model is based on the theory of isotropic turbulence and probability. This model was used in prediction of breakage rate in the current simulation.

3. Numerical implementation

In the current work the hydrodynamics of a laboratory scale cylindrical bubble column initially filled with tap water and with a diameter of 0.172 m and height of 1.7 m was studied. Fig. 1 shows the schematic overview of the investigated column. The mesh structure has important effect in the simulation results. In fact, recirculation of the continuous phase and eddies in the highly turbulent system of cylindrical bubble column requires special treatment for meshing. Moreover, in bubble driven vertical flows, some of the important interfacial forces are very strong in some special geometrical regions like near to the wall. So, it is necessary to consider refined mesh in appropriate regions. Furthermore, according to flow behavior in the current system and in order to have lower computational load, it is recommended to mostly use prism or hexahedral type of meshes.

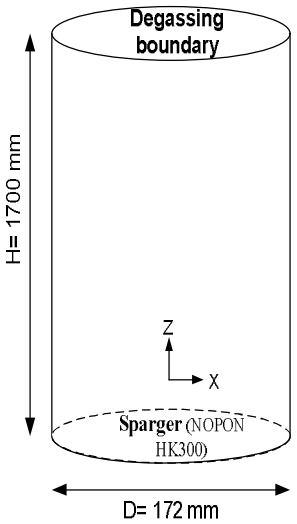

Figure 1- Schematic geometry of the laboratory scale cylindrical bubble column

In order to save calculation time a 5 degree slice of the column was simulated. The mathematical models and closures were solved by using the coupled solver in ANSYS CFX 10. This solver is based on the simultaneous solution of linearized conservation equations. Some parts of the simulation are done by implementing FORTRAN codes in the commercial software. Calculations were performed on an Intel P4 3.4 GHz processor with 2 GB RAM. In the simulations the column is initially full of stagnant water and gas is evenly fed from the bottom with different superficial velocities. Based on the results of photographical measurements, bubble sizes are assumed to be in the range of 3 to 8 mm. Homogenous distribution of bubble sizes was assumed as boundary condition at the sparger. Moreover, the population balances for the different discretized bubble size groups were solved by using the MUSIG model and by considering the Prince and Blanch and Luo and Svendsen models for coalescence and breakage, respectively. Furthermore, the liquid can not leave the geometry whereas air is able to escape from the free surface. This is modeled by using degassing boundary condition through the free surface of the liquid. According to this condition, gas is the only phase which can go out from the domain and an artificial wall will be assumed for the liquid phase.

In order to have better agreement with the experiments some of the important model parameters should be defined and adjusted in the software. The different drag and non-drag models and coefficients were implemented by using the expression language or FORTRAN codes.

4. Experimental setup

Measurements were carried out by PIV. The equipment was provided by LaVision GmbH. Fig. 2 shows a schematic view of the experimental setup. Gas was fed to the column through a flexible rubber plate sparger (NOPON HK300), which produces a steady homogeneous flow of small bubbles. The used superficial gas velocities in the inlet were 0.36 and 0.72 cm/s. Further details of the experimental implementation are described in Laari et al. (2006). The time-averaged liquid, bubble and slip velocity distributions accompanied by the turbulent kinetic energy distribution are some results which were obtained by PIV. Comparison of the simulated and experimental results is carried out in the following chapters.

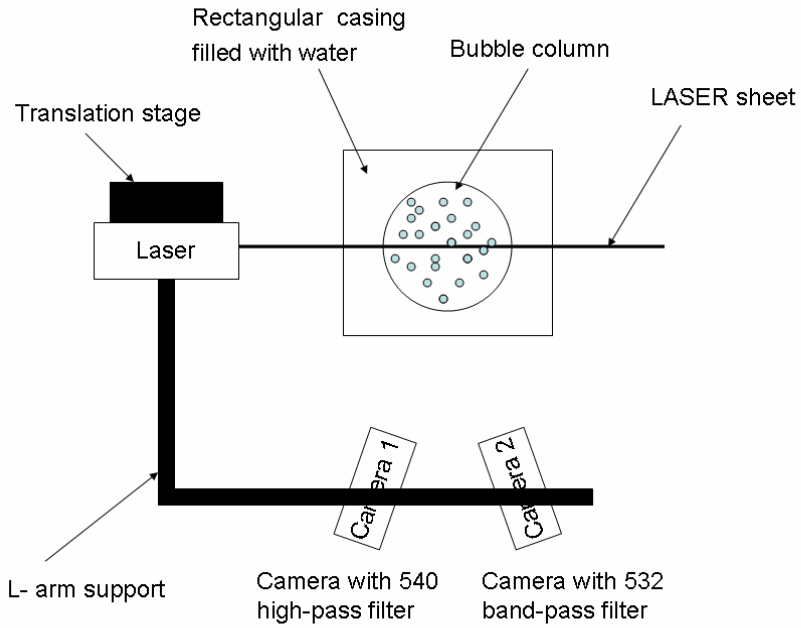

Figure 2- Experimental bubble column two-phase PIV setup (view from top).

5. Results and discussion

The gas-liquid flow in a laboratory scale cylindrical bubble column was simulated by ANSYS CFX 10. The calculations were carried out for two different superficial gas velocities of 0.36 and 0.72 cm/s in the inlet. The influence of the different interfacial force closures on flow fields and bubble size distribution in the column was investigated by implementing three different closures in the simulations as described in Table 1.

5.1. Velocity field investigation

Figures 3 to 5 show the velocity distributions for water, air and slip obtained by the implementation of two different interfacial closures (A, B) in the simulation. Figures 7 to 9 show the same fields for the higher superficial gas velocity (Vg=0.72 cm/s).

Comparison of the simulations and the experimental results show that the closures A and B can predict the velocity field with reasonable accuracy in magnitude and direction. Indeed, closure C, which is based on the experimental model of Ishii and Zuber (1979), has also good agreement with the PIV results, especially at the lower superficial gas velocity in the inlet. A more quantitative comparison between the different closures can be obtained from Figs. 6 and 10. These figures present how well the liquid, gas and slip velocity field in a particular height can match with the experimental data. As it is clear from the figures the interfacial closure B predicts lower liquid and gas velocity in most of the regions. Nonetheless, the accuracy of all closures seems to be in the same order of magnitude.

From these figures it is apparent that the direction of the liquid flow is upward in the center and downward near to the wall, which describes the circulation of water in a physically acceptable way. As a matter of fact, this direction is due to circulation of liquid from the highly turbulent regions in the core to the regions were the total interfacial force is lower. Moreover, proper boundary condition for the liquid free surface is crucial to obtain meaningful results and a correct circulation pattern. Since the simulation was conducted in unsteady state conditions these results are obtained by field averaging over time. The time averaging starts when the average residence time of bubbles in the column is passed. Before that, liquid vortices randomly spread in the column and the flow field variables can not be reliably used for averaging. The study shows that stable solution is obtained only in transient simulation mode.

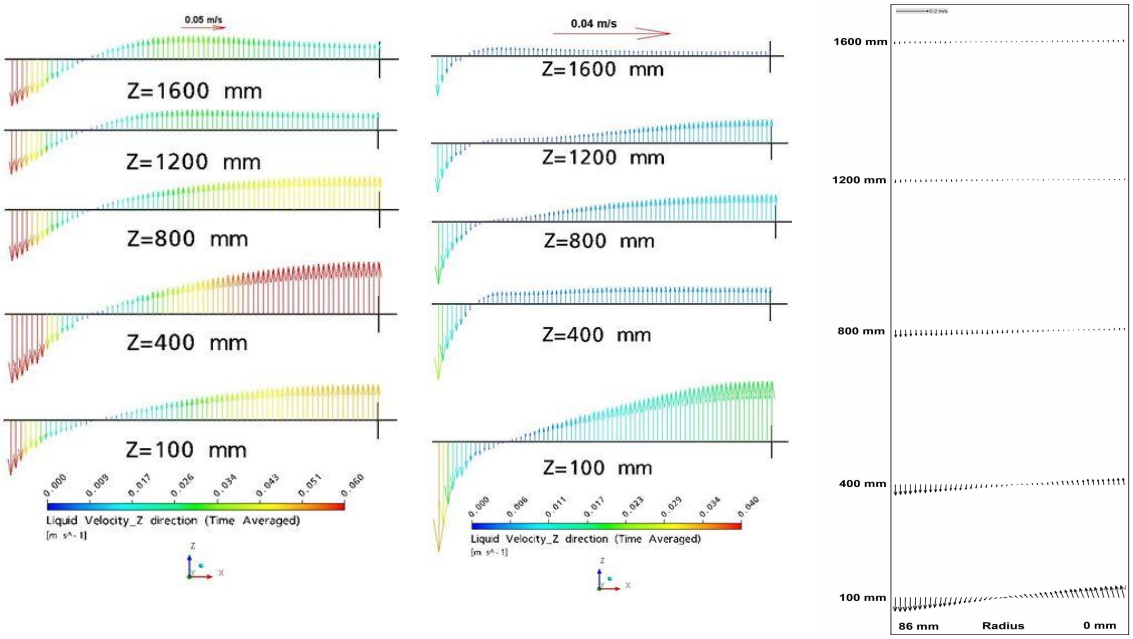

a) b) c)

Figure 3- Time-averaged liquid velocity vectors in different heights obtained by a) Interfacial closure A b) Interfacial closure B and c) PIV. Inlet superficial gas velocity Vg=0.36 cm/s, System: Air/tap water

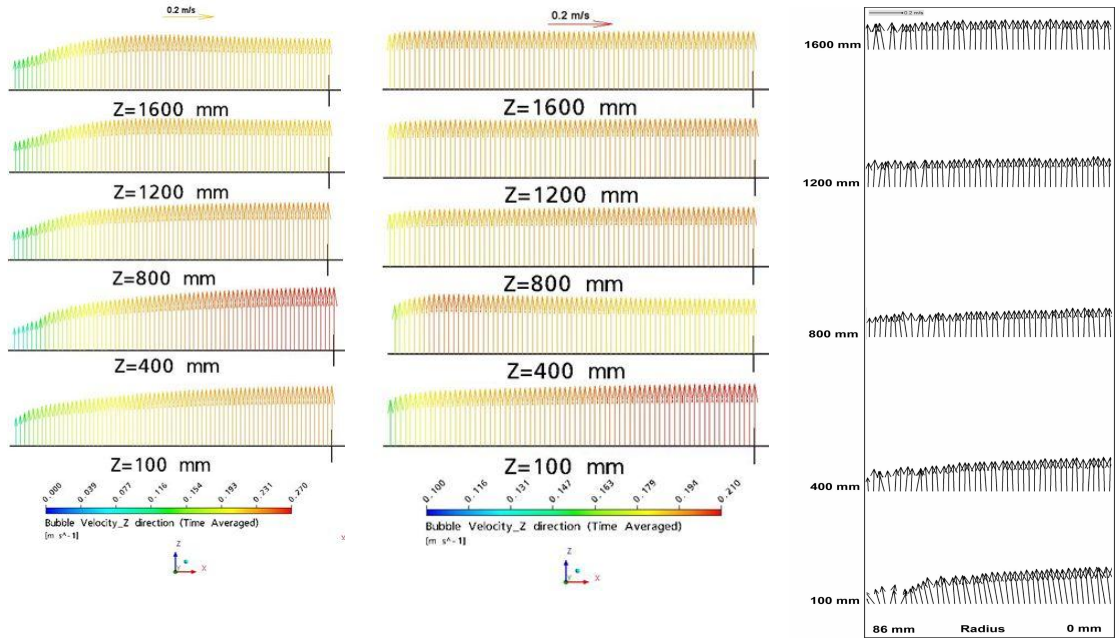

a) b) c)

Figure 4 -Time-averaged gas velocity vectors in different heights obtained by a) Interfacial closure A b) Interfacial closure B and c) PIV. Inlet superficial gas velocity Vg=0.36 cm/s, System: Air/tap water

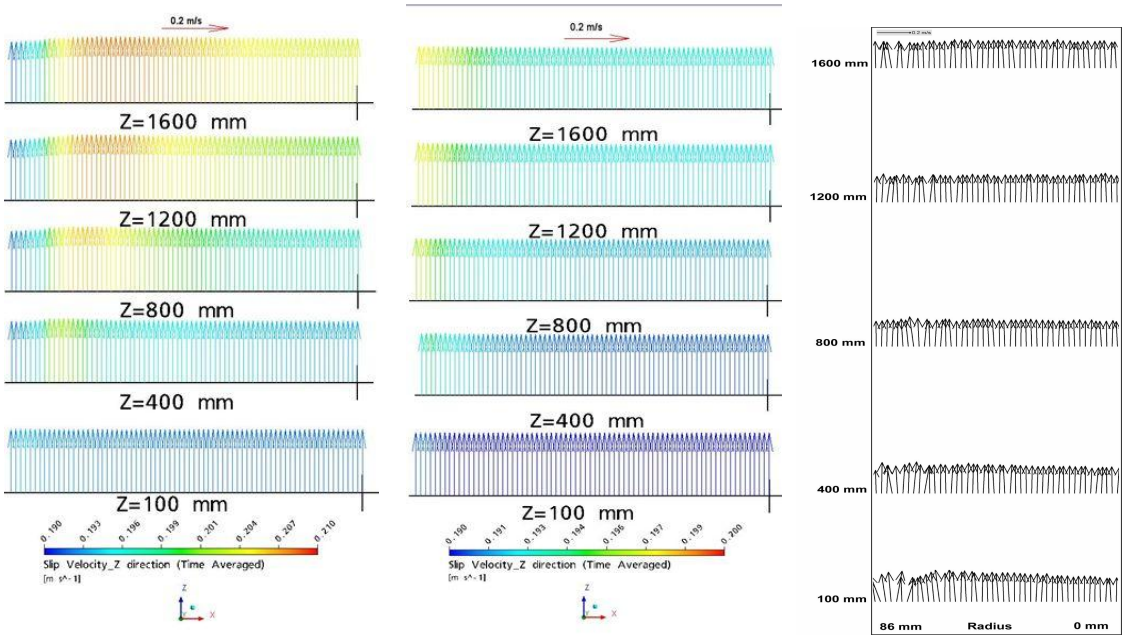

a) b) c)

Figure 5-Time-averaged slip velocity vectors in different heights obtained by a) Interfacial closure A b) Interfacial closure B and c) PIV. Inlet superficial gas velocity Vg=0.36 cm/s, System: Air/tap water

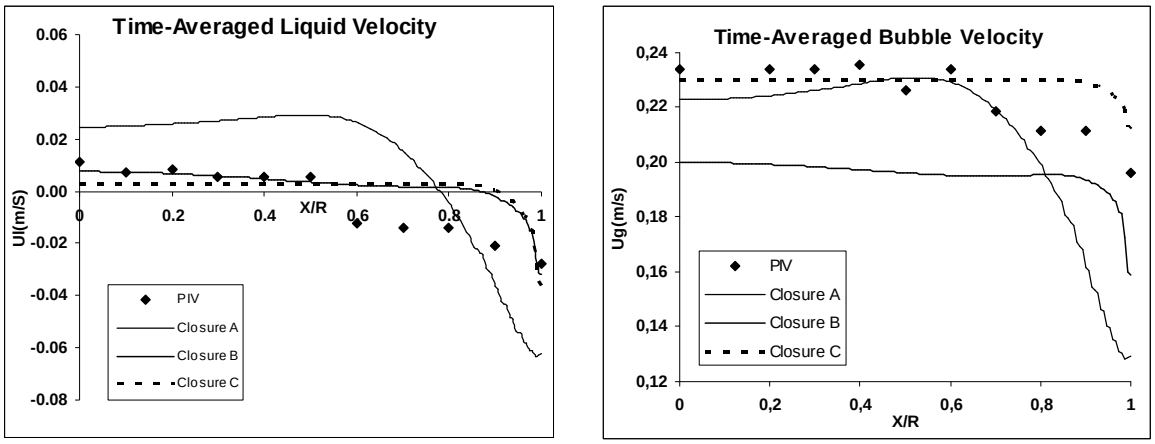

Figure 6- Comparison of experimental time-averaged vertical liquid and gas velocities obtained by PIV with simulation results gained by three different closures.(Z/H =0.7, Inlet superficial gas velocity 0.36 cm/s, System: Air/tap water)

It is generally suggested to consider bubble dependency in the interfacial closure formulation. This investigation shows that this dependency is quite important in getting reliable results for flow fields, hold up, bubble size distribution and also for turbulence. For the velocity fields, the magnitude and direction of the vectors can be affected remarkably. Current commercially implemented MUSIG model considers only one flow field for all the bubble size classes. This means that only one set of momentum equation is solved. This will cause some difficulties considering the

dependency from bubble size in the interfacial forces. In order to improve the accuracy it is suggested to use more dispersed phases in the calculations. Each dispersed phase should cover a small range of bubble sizes where the interfacial forces are constant. Accordingly, different size dependent closures can be formulated for each dispersed phase which will lead to various set of momentum equations. Theoretically, the higher the number of dispersed phases the more accurate the flow fields can be. However, the usage of more phases will increase the calculation time remarkably. In addition to the velocity magnitude it can also affect the radial position where the liquid velocity changes its direction in various heights.

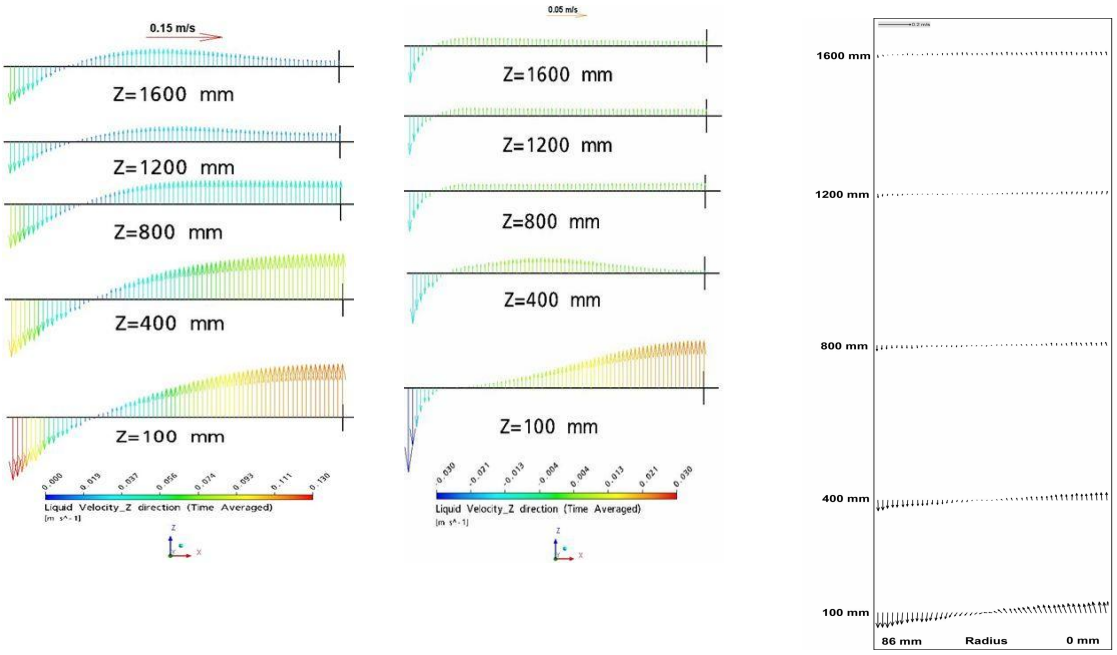

a) b) c)

Figure 7-Time-averaged liquid velocity vectors in different heights obtained by a) Interfacial closure A b) Interfacial closure B and c) PIV. Inlet superficial gas velocity Vg=0.72 cm/s, System: Air/tap water

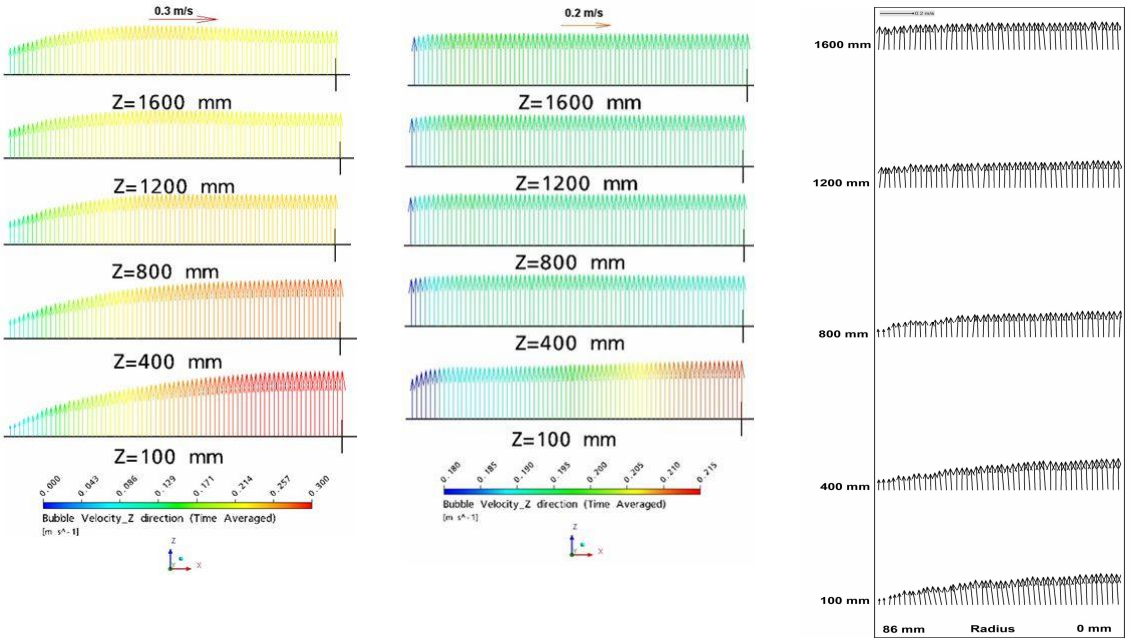

a) b) c)

Figure 8-Time-averaged gas velocity vectors in different heights obtained by a) Interfacial closure A b) Interfacial closure B and c) PIV. Inlet superficial gas velocity Vg=0.72 cm/s, System: Air/tap water

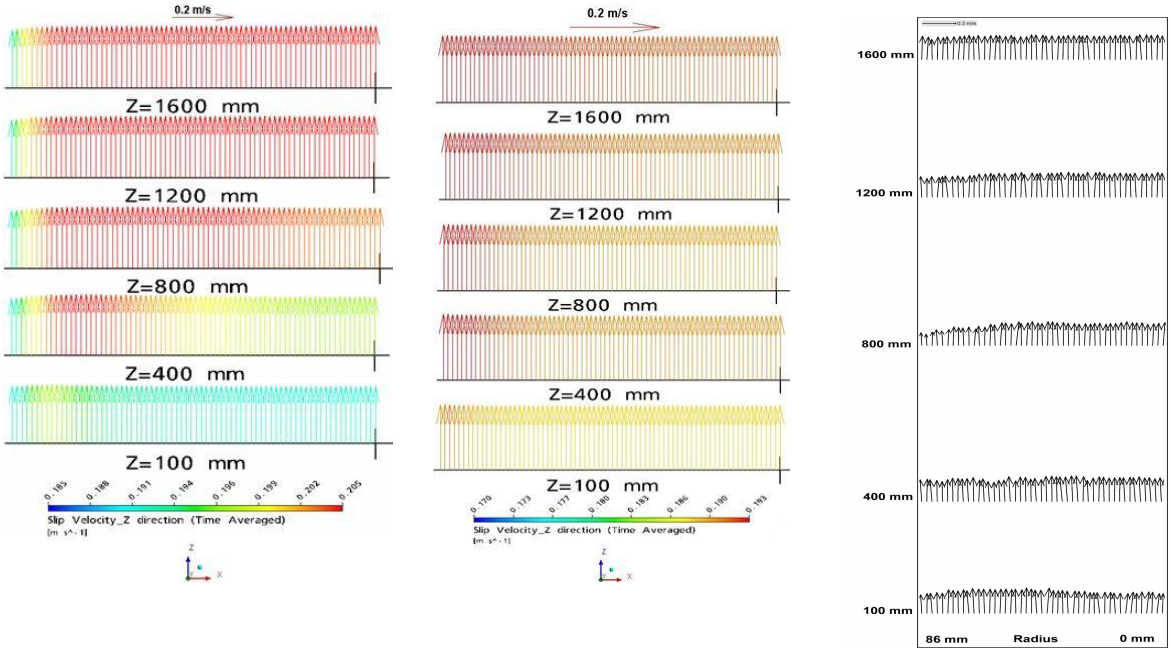

a) b) c)

Figure 9-Time-averaged slip velocity vectors in different heights obtained by a) Interfacial closure A b) Interfacial closure B and c) PIV. Inlet superficial gas velocity Vg=0.72 cm/s, System: Air/tap water

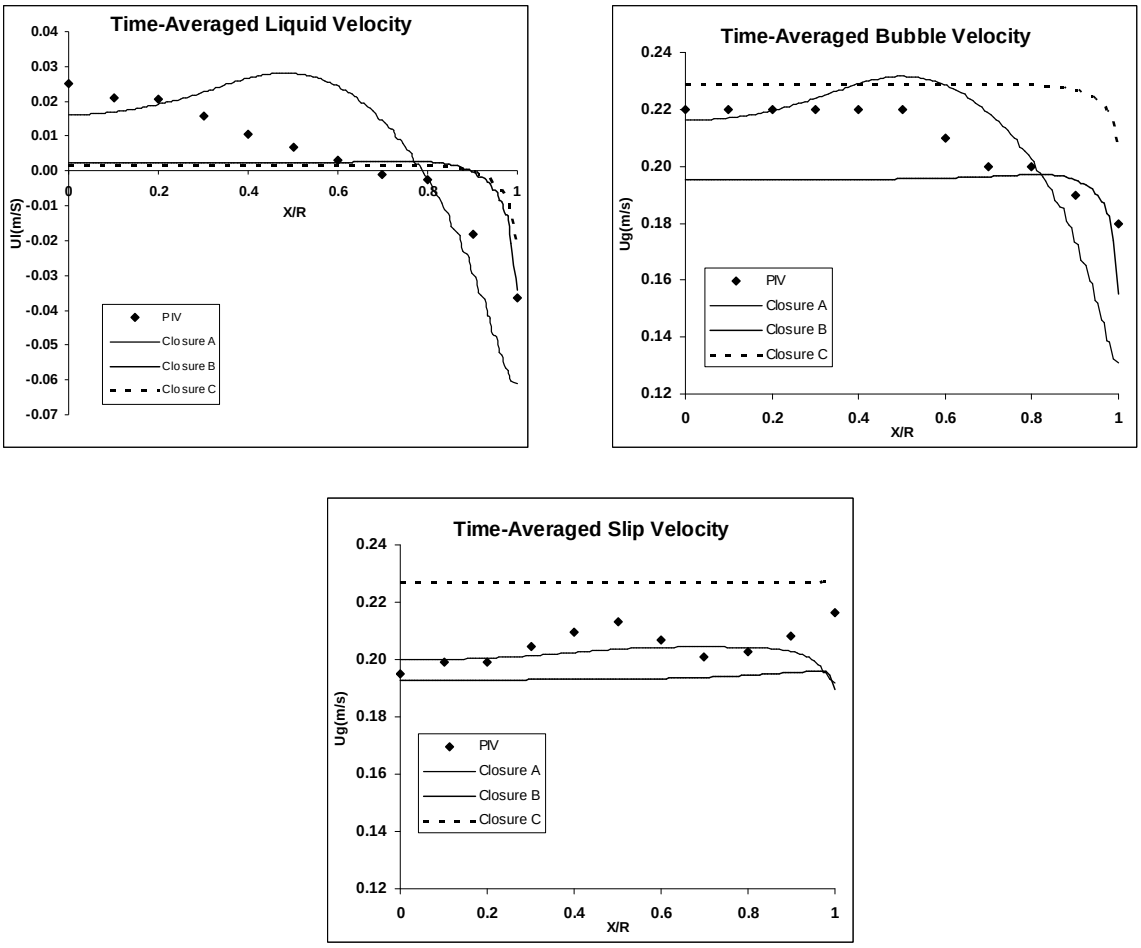

Figure 10- Comparison of experimental time-averaged liquid, gas and slip velocities obtained by PIV with simulation results gained by three different closures. (Z/H =0.7, Inlet superficial gas velocity 0.72 cm/s)

As was mentioned before, the effect of the drag model and the drag coefficient seems to be very important for proper calculation of the hydrodynamics. This effect is mostly observable in the liquid velocity distribution along the column. However, it is not only the drag which can affect the flow fields. The current study shows that the incorporation of only the drag force in the simulation will diminish almost all transversal spreading of bubbles in the column. This causes some inaccuracy to the prediction of the liquid and gas velocity distributions in the column compared to PIV results. This is shown by the strong peak in the predicted liquid velocity at the centreline. The same observation was reported by Deen (2001). Addition of virtual mass to the drag will only gradually lower the strong peek of the liquid velocity in the centre, but the overall behaviour is basically the same. When both the drag and the lift force are included in the simulation, the radial distribution of velocity vectors are more reasonable compared to the PIV results. Slightly more accurate velocities can be obtained by including the virtual mass force in the calculation. However, the inclusion of virtual mass force causes some convergence problems increasing the computation time remarkably.

The correlation of Laurrien et al. (2004) seems to give better prediction compared to Wijngarden (1976). This correlation gives good approximation for the systems with void fraction lower than 40 %. It means that in the current work with void fraction lower than 5 % it should give good prediction. However, inclusion of this equation made a lot of divergence in the calculations increasing the calculation time drastically. On the other hand, it could only make small improvement in the prediction of the flow. Accordingly, it is recommended to include this model only in the cases where the influence of the virtual mass force is strong. Highly accelerated systems, for which the simulation does not lead to quasi-steady state conditions, are systems for which the inclusion of this correlation is expedient.

Moreover, it was observed that the wall lubrication force has important effect on the upward bubbly flow, particularly in thin layer (lower than 5 bubble diameter) adjacent to the wall. Thus, the incorporated coefficients of the Antal et al. (1991) model were selected on the basis of validity near to the wall. The wall lubrication force together with the lift force are the most important forces which mainly determine radial gas volume fraction and interfacial area distribution in the near wall regions of column. In situations where small bubbles are pushed towards the wall by the lift force, the wall lubrication force acts in the opposite direction to ensure that bubbles are not accumulated at the wall. In fact, if this force is not considered wrong void fraction and liquid velocity profile, particularly in adjacent to the wall, will be obtained. In order to truly consider the effect of this force, the mesh structure should consist of refined mesh at least in the distance equal to 5 times of maximum bubble size.

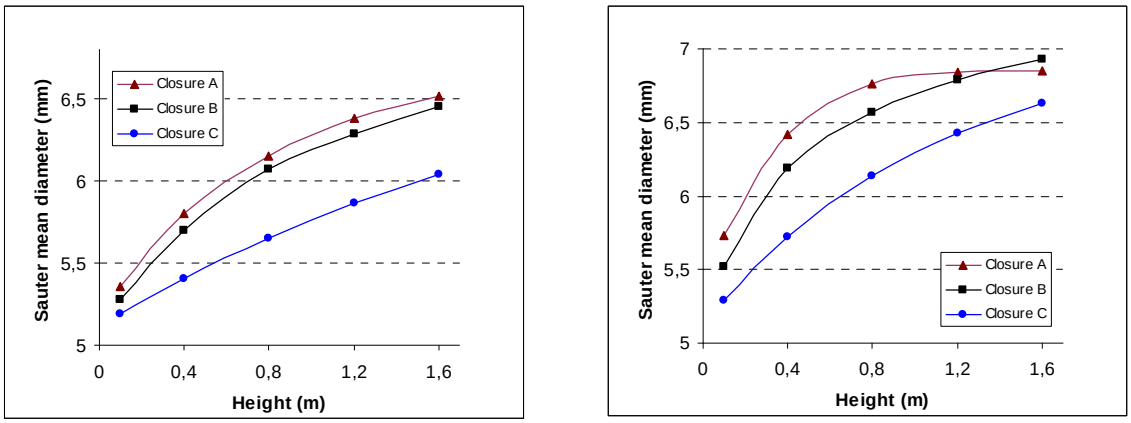

a) Ug= 0.36 cm/sec b) Ug=0.72 cm/sec

Figure 11- Time and cross-sectional area averaged bubble Sauter mean diameter (mm) predicted by the different interfacial force closures in various vertical positions in the column (System: Air/Tap water)

Further investigations of the bubble size distribution in the column shows that the bubble size increases along the column. This fact can be concluded from the distribution of the time-averaged bubble Sauter mean diameter shown in Fig. 11. This happens due to coalescence in higher positions. Indeed, it is more likely that larger bubbles intend to move towards the centre line and rise from there to the free surface while smaller bubbles show the opposite behaviour. A plausible explanation for this is that the bubbles with Eo>4 will have a negative lift coefficient which will

push them towards the centre. Conversely, bubbles with Eo<4 will move to the wall as a result of positive lift coefficient.

The different closures give different prediction for the Sauter mean. Fig. 11 shows that closure A predicts slightly higher Sauter mean than the others. However, there is not much difference in the magnitude of the mean diameters. Moreover, comparison of Figs 11-a and 11-b shows that higher gas velocity in the inlet leads to large Sauter mean values in the column

5.2. Turbulent kinetic and eddy dissipation rate study

The distribution of the time-averaged water turbulent kinetic energy in the different regions of column is shown in Fig. 12

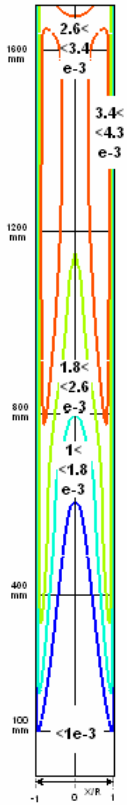

Figure 12- Time-averaged water turbulent kinetic energy [m^2 S^-2] in the column (closure A, Vg=0.36 cm/s)

As shown in this figure, the level of the turbulent kinetic energy is highest in the off centre regions on the top of the column. This means that stronger water velocity fluctuations are traced in those regions. However, the study shows that the different interfacial closures (A, B and C) can create different distributions. Furthermore, investigations show that the consideration of the active surface of the sparger in the geometry can give better predictions for kinetic energy distribution along the column. By an example, inactive areas in the sparger can cause uneven bubble distribution in the inlet. Hence, gas is fed to the column through fewer active holes of the sparger

giving higher superficial gas velocity at the inlet contrary to the simulated case. In fact, in bubble driven flows this can have more impact on the hydrodynamics of the system causing more velocity fluctuations in some regions.

The distribution of the simulated turbulent energy dissipation rate (epsilon) in the domain is almost similar to the turbulent kinetic energy, as shown in Fig 11. The order of magnitude for the predicted energy dissipation rate is lower than the total power input per unit mass of liquid calculated from the work done by the gas rising from the bottom to the free surface on the top of the column. It may be concluded that the k-epsilon model seems to predict lower epsilon values with respect to total power input.

6. Conclusion

Results of 3D transient simulation of a laboratory scale two phase bubble column are presented. The effect of the interfacial momentum exchange terms were examined by different drag and non-drag force models. In the non-drag forces the effect of lift, turbulent dispersion, virtual mass and wall lubrication forces on the time-averaged liquid, slip and bubble velocity and gas hold up were studied. The validated simulation results by PIV measurements show that the drag, lift and turbulent dispersion forces are the most important momentum transfer terms in the model. However, the effect of the wall lubrication force is also considerable. Slightly more accurate results can be obtained by including the virtual mass force to the calculation. However, the inclusion of the virtual mass force causes some convergence problems increasing the computation time remarkably. The study shows that appropriate drag model has crucial effect on the hydrodynamics of the column. Moreover, the effect of the bubble size on the lift force should be considered. This behaviour can affect the radial gas hold up distribution and also the water velocity distributions in the column. This can be concluded from the bubble size distributions along the column. Study of different interfacial closures (details of the formulas in Table 1) show that closure A (based on the Jakobsen drag model (1997) and on the non-drag forces of various authors) and closure B (based on the Tomiyama closure (2004)) had better prediction of the hydrodynamics. However, the turbulent kinetic energy and eddy dissipation rate predicted by closure B and closure C (based on the Ishii and Zuber (1979) model) was lower than expectations. The study shows that the consideration of proper sparger geometry can help to give more experimentally acceptable distributions for turbulent kinetic energy in the column. Even though the effect of the interfacial forces in the simulation of bubbly flow is quite important there is currently no universal interfacial closures for these systems. It was found that geometry, boundary conditions and material properties can affect the selection of interfacial force closures considerably.

Notation

a	[m^2/m^3]	Specific interfacial area
B	[$1/m^3s$]	Birth rate
C		coefficient
d	[m]	diameter
d_{32}	[m]	Sauter mean diameter
D	[$1/m^3s$]	Death rate
E	[]	Mean aspect ratio (detail in Tomiyama, 2004)
Eo	[]	Eotvos number
f_i	[]	Bubble size fraction of group i in each dispersed phase
g	[m/s^2]	Gravity
k	[m^2/ s^3]	Turbulent kinetic energy
M	[N]	Interfacial force
n	[$1/ m^3$]	Population density
N_c	[]	Number of size class
P	[Pa]	Pressure
Si	[kg/m^3s]	Source for continuity or scalar equation
U	[m/s]	Velocity
V_g	[m/s]	Gas Superficial Velocity in the inlet
y_w	[m]	Layer thickness in Antal model

Greek Letters

α		Phase Volume Fraction
μ_{eff}	[kg/ms]	Effective viscosity
ρ	[kg/m^3]	Density

Subscript or Superscript

B	Breakage
C	Coalescence
D	Drag
g	Gas
i	Size class counter
k	Phase
l	Liquid
L	Lift
p	Particle
TDF	Turbulent dispersion force
VM	Virtual Mass Force
w1,w2	Index for Antal model coefficients
WL	Wall lubrication Force

Mathematical operators

D/Dt	Substantial derivative
∇	The “del” operator
$\frac{\partial}{\partial t}$	derivative

References

Antal, S., Lahey, R., and Flaherty, J. , *Int. J. Multiphase Flow*, 7, p. 635, 1991.

Buwa, V. V., Ranade, V. V., *Chemical Engineering Science*, 57, 4715-4736 ,2002

Clift, R., Grace, J.R., Weber, M.E. , *Bubbles, Drops and Particles*. Academic Press, New York, 1978

Darmana, D., Deen, N.G., Kuipers, J.A.M. , *Chem. Eng. Sci.* 60, 3383–3404, 2005

Deen, N., *PhD thesis*, Aalborg University, Denmark, Aug. 2001

Delnoij, E., Kuipers, J.A.M., Van Swaaij, W.P.M. , *Chem. Eng. Sci.*, 52, 3759–3772., 1997

Ishii, M., Zuber, N., 1979., *A.I.Ch.E. Journal* 25, 843–855, 1979

Jakobsen, H.A., et al., *Ind. Eng. Chem. Res.*, 36, 4052-4074, 1997

Krishna, R., Urseanu, M.I., van Baten, J.M., Ellenberger, J., *Chem. Eng. Sci.*, 54, 4903–4911, 1999.

Krishna, R., Urseanu, M.I., Van Baten, J.M., Ellenberger, *Chem. Eng. Sci.*, 55, 3275, 2000

Laari A., Turunen I., Sha Z., *Chisa conference*, Prague, Chek republic, 2006

Laurrien, E., Niemann, J., *5th International Conference on Multiphase Flow*, ICMF'04, Yokoham, Japan, May 2004

Lehr, F., Milies, M., Mewes, D., *AICHE J*. 48,2426,2002

Lo S. , *AEAT-1096, AEA Technology*,June 1996.

Lopez de Bertodano, M., *PhD Thesis*, Rensselaer Polytechnic Institute, Troy New York, 1991.

Luo, H., Svendsen, H., *AIChE. Journal* , 42, 1225–1233, 1996

Lucas, D., Krepper, E., Prasser, H.-M, *Int. J. Thermal Sci* , 40, 217-225, 2001

Pan, Y., Dudukovic, M.P., Chang, M., *Chem. Eng. Sci.* , 54, 2481–2489, 1999.

Prince, M.J., Blanch, H.W., *AIChE Journal*, 36, 1485–1499, 1990

Sato, Y. , Sekoguchi, K., *Int. J. Multiphase Flow*, 2, p.79, 1975.

Sha Z. Laari A. Turunen I., *Chemical Engineering & Technology*, Volume 29,

Issue 5, Pages: 550-559, 2006

Sokolichin, A., Eigenberger, G., Lapin, A., Lubbert, A., *Chem. Eng. Sci.* 52 (4), 611–626, 1997

Sokolichin, A., Eigenberger, G., *Chem. Eng. Sci.* ,52, 611–626, 1999

Sokolichin, A., Lapin, A., Eigenberger, G., *AICHE,* Vol. 50, No. 1, 2004

Tomiyama, A., *3rd Int. Symp. On two-phase Flow*, Italy, 22-24 Sep., 2004

Torvik, R., Svendsen, H.F., *Chem. Eng. Sci.* 45, 2325–2332, 1990.

Van den Hengel, E.I.V., Deen, N.G., Kuipers, J.A.M., *Ind. Eng. Chem. and Res.* 44, 5233–5245, 2005.

Wiemann, D., Mewes, D., *Chem. Eng. Sci.*, Vol. 60, 6085-6093, 2005.

Wijingarden, V., *J. Fluid Mech.,* 77,27-44 ,1976

Zhang. D, Deen, N.G., Kuipers, J.A.M, , *Chem. Eng. Sci.,* Vol. 61, 7593 – 7608, 2006